Photodissociation Studies of M(Furan)$^+$ (M = Cu, Ag, and Au) and Au(C_3H_4)$^+$ Complexes

Po-Hua Su, Fang-Wei Lin, and Chen-Sheng Yeh*

Department of Chemistry, National Cheng Kung University, Tainan, Taiwan 701, R.O.C.

Received: May 10, 2001; In Final Form: July 27, 2001

The group 11 metal/furan cationic complexes were generated using a laser vaporization technique combined with a supersonic beam expansion in a time-of-flight mass spectrometer. From the viewpoint of the ionization energies, these complexes were treated as Cu^+−furan, Ag^+−furan, and Au−furan$^+$. The photodissociative ligand-to-metal charge transfer with an exclusive furan cation was observed for Cu and Ag, whereas a simple bond cleavage with furan$^+$ formation was inspected for Au. The photofragment spectra were recorded as a function of the laser wavelength. The continuous and structureless bands were measured in each complex. The thresholds of the fragment appearance determined the upper limits of the ground-state binding energy with 37 kcal/mol for Cu^+−furan, 28 kcal/mol for Ag^+−furan, and 62 kcal/mol for Au−furan$^+$. An ab initio approach at the MP2 level was employed to optimize the geometries of the furan complexes and the binding energies were obtained using CCSD(T) single point calculations. The measured binding energies in both Cu and Ag complexes approximate to the theoretical predictions. Both the experimental and theoretical measurements yielded the enhanced bond strength for Au complex. In addition, a furan ring opening process leading to Au^+−C_3H_4 production was observed in the reactions of a gold atom with a furan molecule. The binding energy was taken as a reference to discern three possible isomers, i.e., allene, cyclopropene, and propyne, as C_3H_4 species by means of experimental and theoretical approaches.

Introduction

Because of their importance in biological structures and catalysis, many studies have sought to understand the metal-ion interactions with π-rings of the aromatic metal complexes.[1] The rich data attained on binding energies and geometries have provided the central requisite to characterize metal/ligand interactions. Among the aromatic molecules, benzene is perhaps the most studied system. In addition to benzene, aromatic heterocycles are known to play a vital role in industrial applications, such as petroleum refining and coal liquefaction, and the five-membered heteroaromatic rings are recognized as an important class of compounds.[2]

Although extensive work has been performed on the metal-cation interactions with the benzene ligand, the complexation of heterocycles with metals has received little attention in the gas phase.[3−7] The five-membered heterocycles ligation with metals exhibits a variety of binding modes, e.g., η^1-, η^2-, η^3-, η^4-, and η^5-bound.[3,5,6] Dunbar and co-workers experimentally and theoretically investigated the binding energies and geometries for a number of main-group and transition-metal cations coordinated with pyrrole complexes.[6] Their results showed the metal ions lying over the pyrrole ring. Stöckigt performed ab initio and density functional calculations on Al^+−furan (C_s) and Al^+−pyrrole (C_s).[5]

In our continued efforts to investigate the ion complexes containing metal and heterocyclic molecules in the gas phase, the furan molecule was selected for this study. Furan has large electronegativity of the heteroatom oxygen, thus it was suggested to have a preferential formation of σ-bonds to metal centers instead of forming π-complexes.[8] Stöckigt calculated Al^+−furan and obtained stronger bond strength in complex with π-bound formation.[5] Experimentally, Freiser and co-workers determined the binding energy as 57 kcal/mol for Co^+−furan via a photodissociation technique by observing the Co^+ fragment.[4] Recently, we measured the photofragment spectrum of Ag^+−furan and the upper limit on the bond strength was derived from the threshold of the photodissociative charge-transfer furan$^+$ channel.[7] In this report, photodissociation methodology was employed to achieve the upper limits on the Cu^+−furan and Au−furan$^+$ in addition to Ag^+−furan. Moreover, an intense peak assigned as Au^+−C_3H_4 produced from the ion source was studied, as well. Ab initio calculations were also used to give a picture of the geometric structures and binding energies for these species.

Experimental Section

The details of the experimental setup were described previously.[9] The ion complexes were generated using a laser vaporization method combined with a supersonic molecular beam source. A copper (99.999%) or silver (99.9%) rod was suspended in a cutaway holder, a rod holder without a growth channel to produce primarily complexes containing one and/or two ligands. For gold complex production, gold foil (99.9%) was wrapped around an Al rod. The rotating and translating rods were irradiated using a 532 nm wavelength of the second harmonic output from an Nd:YAG laser operated at 10 Hz with 1−2 mJ/pulse. The vaporization laser beam was focused 1.5 cm in front of the metal rods. Prior to seeding furan vapor, pure He gas (6 atm) was used to inspect the ion products from our ion source. It was found that only Cu^+, Ag^+, and Au^+ atomic signals appeared, and that no other impurities, such as metal oxides, were detected. He gas carried the furan vapor, where furan was loaded into a liquid reservoir, into a pulsed valve and expanded, followed by intersection with metal ions at the vaporized region. The ion complexes were then skimmed into

* Author to whom correspondence should be addressed. Fax: +886-6-2740552. E-mail: csyeh@mail.ncku.edu.tw.

10.1021/jp011799j CCC: $20.00
Published on Web 09/29/2001

a reflectron time-of-flight mass spectrometer and were mass-selected for carrying out photodissociative performance. To isolate the metal ion complexes, two parallel plates serving as a mass gate were located inside the flight tube. When the desired ion packet reached the mass gate, the positive voltage was pulsed to ground for ions to pass through and traveled along the field-free tube. In the photodissociation experiments, an unfocused dissociation laser crossed the mass-selected ions at the turning point in the reflector. The fragment and parent ions were analyzed from their flight times. The dissociation laser was a pulsed tunable dye laser (Continuum ND6000) pumped by an Nd:YAG laser (Continuum Surelite). The wavelength-dependent spectra were measured as the intensities of the fragments relative to the dissociative laser wavelength.

Theoretical Computations

The calculations were performed using the second-order Møller−Plesset perturbation theory (MP2). The double-ζ valence basis sets and the effective core potentials (ECPs) of Hay and Wadt were used for Cu, Ag, and Au atoms[10] and the 6-31G-(d, p) set was selected for C, H, and O. The relativistic effects were included in the Hay-Wadt ECPs of Ag and Au. We also added the f polarization functions to increase the flexibility of the ECP basis set. The f exponents are 3.525 for Cu, 1.611 for Ag, and 1.050 for Au.[11] The geometries of the ligands and ion complexes were fully optimized at the MP2 level, whereas the zero-point energy corrections evaluated from the harmonic vibrational frequencies obtained at the MP2/6-31G(d, p) level. CCSD(T) single point calculations with the corresponding MP2/6-31G(d, p) zero-point energies were derived from CCSD(T)/6-31G(d, p)//MP2/6-31G(d, p). The calculations were performed using the Gaussian 98 suite of programs.[12]

Results and Discussion

Cu^+−Furan, Ag^+−Furan, and Au−$Furan^+$. The mass distributions of the Figure 1 display the associated products containing metals in addition to the bare atomic signals. The doublet patterns observed for the copper and silver mass spectra arose from the isotopes of 63 (69.1%) and 65 (30.9%) for Cu and 107 (51.5%) and 109 (48.2%) for Ag, whereas gold has mass 197 with 100% abundance. The experimental conditions were adjusted to give the intense ion complexes with one ligand ligation. In the case of the copper and silver complexes, a simple condensation reaction occurred with furan molecules coordinated with metal ions. From the viewpoint of the ionization energies (IEs), the positive charge should localize on the Cu (IE = 7.72 eV) and Ag (IE = 7.58 eV) as compared with the IE value (8.89 eV) on the furan molecule.[13,14] Interestingly, an ion−molecule reaction with the formation of C_3H_4 (m/z = 40) ligation with Au^+ took place as well as the associated furan complexes observed in the gold reactions with furan. Here, we will refrain from a discussion on the gold reactivity, since the laser ablation introduced to generate metal ions can be formed in electronically excited states and readily accesses the endothermic pathway relative to the ground-state reactions. Our ion source is not designed to discern such chemical specificity. Although we avoided the metal ion reactivity subject, it seems that gold exhibits higher activity. On the basis of the previous studies in furan pyrolysis, the m/z 40 (C_3H_4) species was the dominant decomposition product and was identified as allene and propyne.[15−19] It was further suggested that the propyne structure was the major channel.[16] Assuming C_3H_4 as allene, cyclopropene, or propyne, these three isomers have IE above 9.6 eV, which is greater than 9.22 eV of gold.[14,20] It is expected that

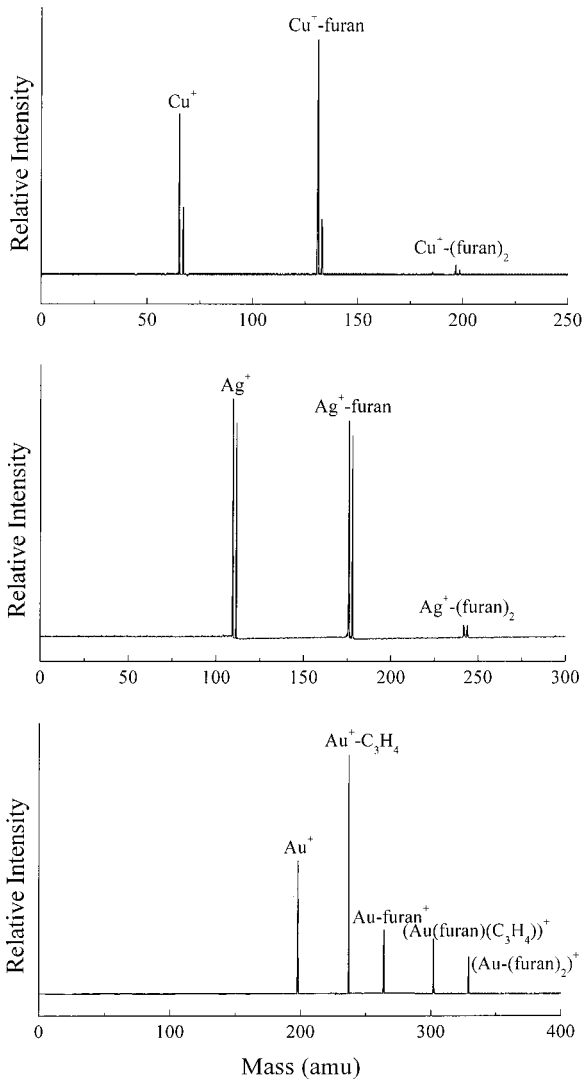

Figure 1. Time-of-flight mass distributions of the metal/furan cationic complexes and the complexation of C_3H_4 with gold.

the ion complexes should have the complexation of Au^+ with C_3H_4. However, the associated furan adduct is viewed as Au−$furan^+$ from the IE difference. If the Au−$furan^+$ complex is formed in our ion source, there is a high possibility that a furan cation is present in the mass spectrum. As a matter of fact, both the $furan^+$ and $(furan)_2^+$ channels could be readily generated in addition to Au−$furan^+$ and Au^+−C_3H_4 when the experimental parameters tuned to lower mass range. We also observed $C_3H_4^+$ peak with a small amount of distribution. No such results mentioned above could be observed in both copper and silver systems. Finally, it was found that Au^+−C_3H_4 always appeared as an intense mass peak as compared to the Au−$furan^+$ signal, implying an efficient furan ring opening process with the C_3H_4 formation.

Figure 2 shows the photodissociation mass spectra of the Cu^+−furan, Ag^+−furan, and Au−$furan^+$ complexes at 355 nm with 9 mJ/cm^2. Both the Cu and Ag complexes revealed the same dissociative behavior with one single fragment liberated from the parents. The daughter ions were assigned as furan molecules. Apparently, the photodissociative action induced intramolecular ligand-to-metal charge transfer for Cu and Ag complexes. With the same laser fluence, photodissociation of Au−$furan^+$ resulted in loss of neutral Au, leading to $furan^+$ and $C_3H_4^+$ channels. The $furan^+$ fragment could be yielded as low as 0.5 mJ/cm^2 of laser fluence while the laser energy should

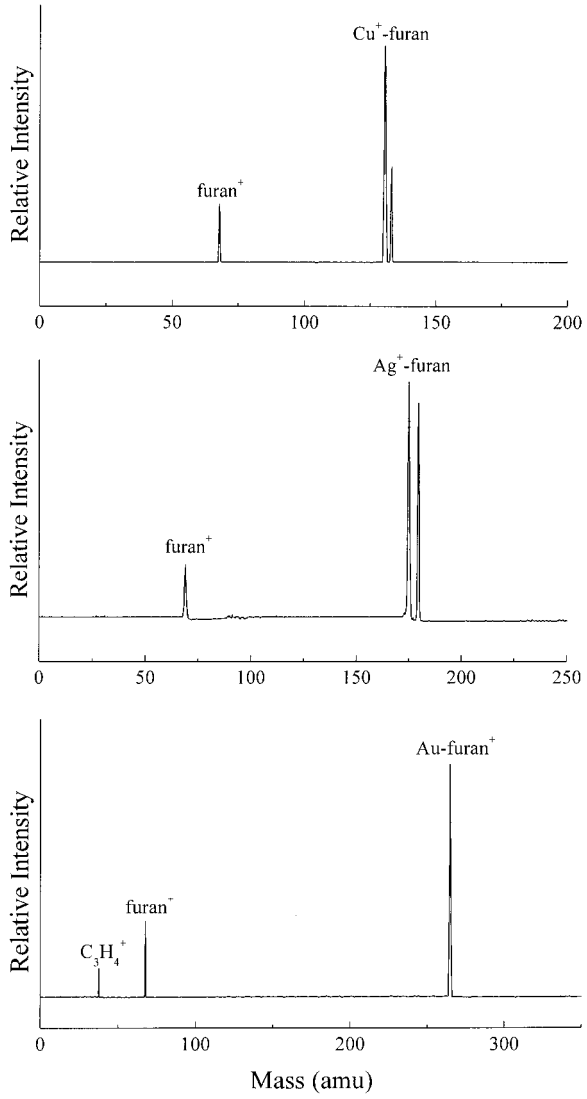

Figure 2. Photodissociation mass spectra of the mass-selected metal/furan cationic complexes at 355 nm. The laser fluence was operated at 9 mJ/cm^2 for all three complexes.

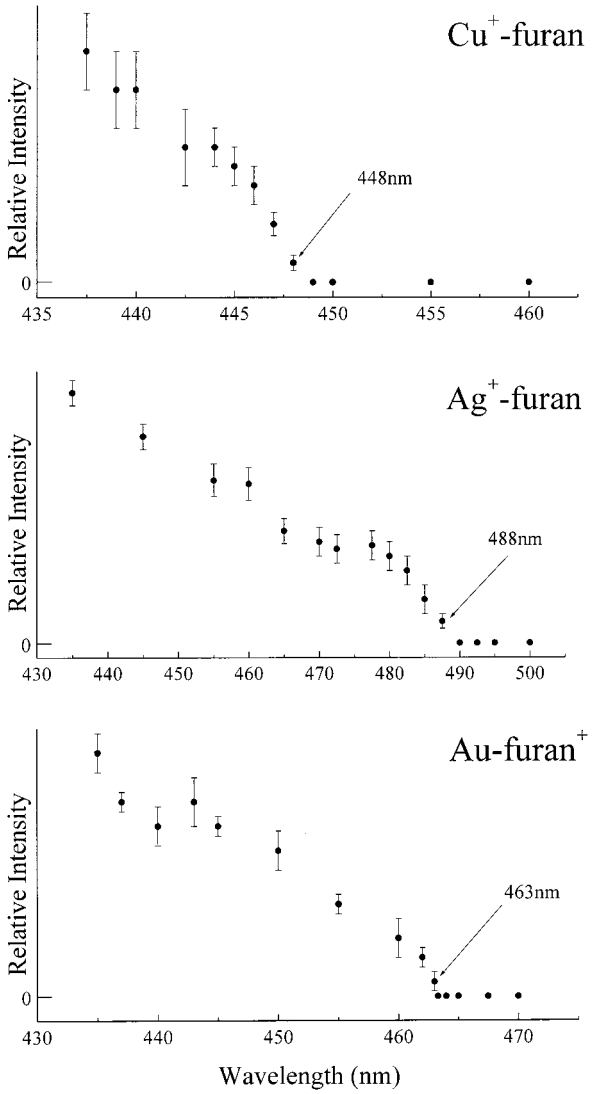

Figure 3. Photofragment spectra of metal/furan cationic complexes. The arrows indicate the thresholds of the fragment appearance.

be tuned up to at least 7 mJ/cm^2 for observing $C_3H_4^+$, indicating a multiphoton mechanism was required to obtain such a product. Since the gold complex is referred as Au−furan$^+$, formation of the furan$^+$ fragment is a simple cleavage in the Au−furan$^+$ bond.

We attempted to search the photodissociation thresholds by monitoring furan$^+$ fragment intensities as a function of the laser wavelength for Cu$^+$−furan, Ag$^+$−furan, and Au−furan$^+$ complexes, as depicted in Figure 3. During the signal search, the parent complexes remained as constant as possible and the laser fluences were kept low (Cu$^+$−furan: 1 mJ/cm^2; Ag$^+$−furan: 1.8 mJ/cm^2; Au−furan$^+$: 3 mJ/cm^2) to minimize multiphoton absorption for recording the wavelength-dependent spectrum. The photodissociation processes were linear with respect to the laser fluences. The error bars in Figure 3 represent the fragment intensity deviations and each data point is an average of two trials. As shown in Figure 3, the onsets, in which the furan$^+$ signals were barely seen, were located at 448 nm for Cu$^+$−furan, 488 nm for Ag$^+$−furan, and 463 nm for Au−furan$^+$. The furan$^+$ intensities continuously increased as the excitation wavelength moved toward the blue, but with no signal below the threshold energies. Due to the limitation of our dye laser facility, the wavelength scan could not be accomplished in the region 430−366 nm. With the observation of furan$^+$ fragments for both Cu and Ag complexes, a reasonable assumption is that the photodissociative charge-transfer behaviors could be attributed to access directly above the dissociation limit of the charge-transfer state. The interpretation of the dissociative mechanism has been restricted within a one-photon excitation. A two-photon excitation cannot be ruled out if the absorption cross-sections are significant difference in two steps, while the power dependence measurement exhibits a linear relation. Figure 4 gives a picture of the asymptote states corresponding to the metal atoms and furan molecule. The lowest excited states correlate to M (^{2}S) + furan$^+$ charge-transfer surfaces, which are 1.17 eV (27 kcal/mol) and 1.31 eV (30 kcal/mol) above the Cu$^+$ (^{1}S) + furan ($^1A_1$) and the Ag$^+$ (^{1}S) + furan ($^1A_1$), respectively. The dissociative charge-transfer may also result from a transition to the higher electronic surfaces, such as that involved in furan chromophore absorption, followed by the electronic curve crossing to the M (^{2}S) + furan$^+$. The furan molecule has a first singlet π-π^* transitions ($^1B_2 \leftarrow {}^1A_1$) beginning near 210 nm.[14] However, excitation of the solvated furan would result in at least 70 kcal/mol solvation energies for both Cu and Ag complexes, which are unlikely to occur in mainly electrostatic complexes. For Au−furan$^+$, a simple cleavage in the Au−furan$^+$ bond could be proceeded by the

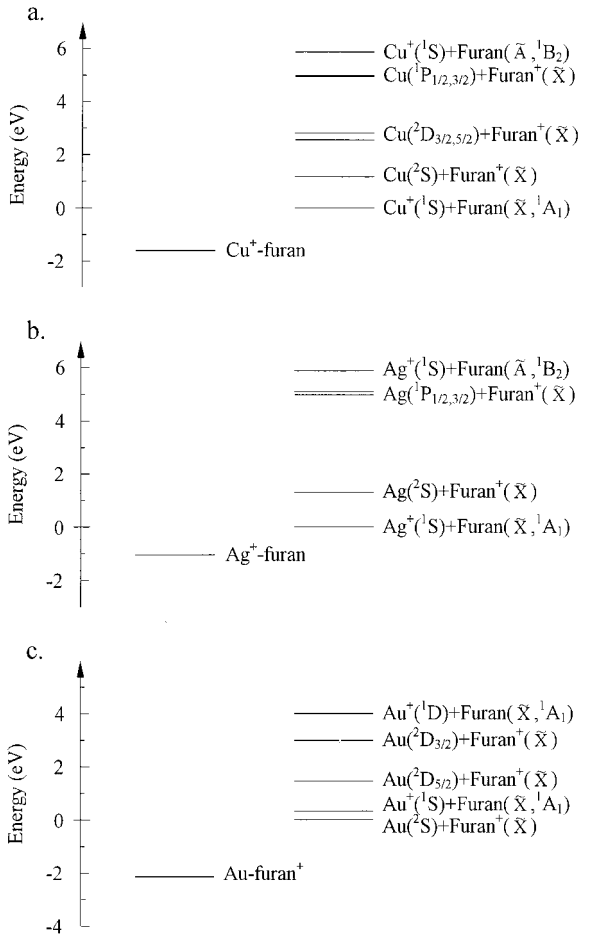

Figure 4. Energetic diagrams showing the asymptote states corresponding to the group 11 metal atoms and furan molecule. The ground-state depths referring to the CCSD(T) predictions.

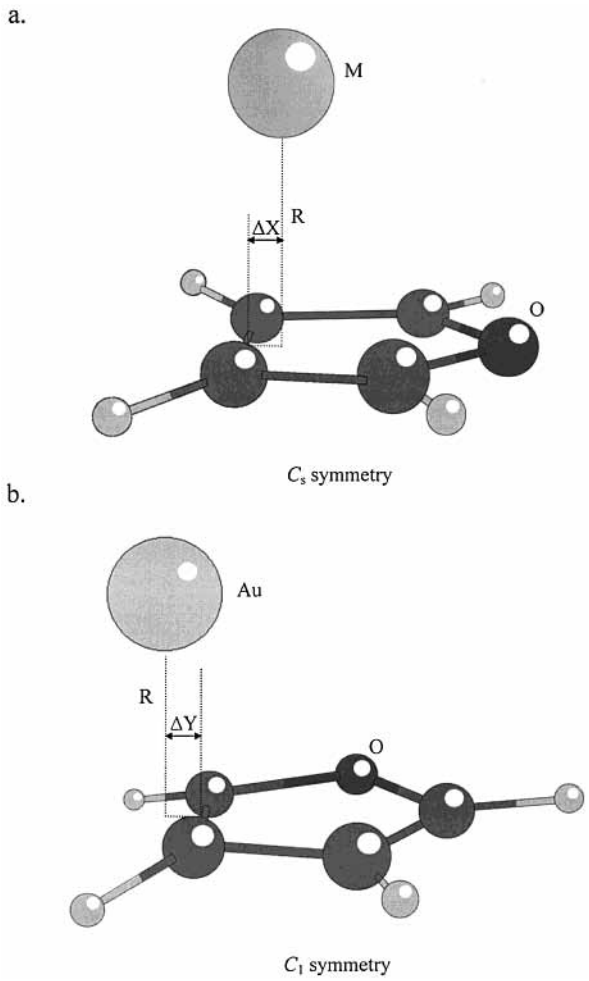

Figure 5. Geometries of the metal/furan cationic complexes, where (a) for Cu and Ag, and (b) for Au.

excess energy over the ground-state dissociation limit or following the multiphoton absorption to the higher electronic excited states, followed by the bond dissociation. However, the calculations shown later on the complex binding energy seem to support a one-photon process leading to bond breakage at the place above the ground-state dissociation limit.

With the measured thresholds in Figure 3, we are able to derive the upper limits of the ground-state binding energies (BDEs) on these three complexes. The charge-transfer action was observed for Cu and Ag species. Taking the determined onsets and the IE difference values between metals and furan molecule, the upper limits of the ground-state bond strengths on the metal−ligand can be attained as following:

$$h\nu \geq D_o'' + \Delta IE$$

This relation allows us to confine the upper limits to D_o'' (Cu^+−furan) ≤ 37 kcal/mol and D_o'' (Ag^+−furan) ≤ 28 kcal/mol. For Au−furan$^+$, the measured threshold gives a straightforward bond strength of D_o'' (Au−furan$^+$) ≤ 62 kcal/mol. The Au complex yields the largest BDE and is at least 25 kcal/mol greater than both the Cu and Ag complexes. A purely electrostatic interaction would have the bond strength decreased from copper to gold. The increased BDE (Au−furan$^+$) could possibly be attributed to the relativistic effects. It is known that gold has the most pronounced relativistic effect throughout the periodic table.[21] Relativity causes a significant contraction of the gold 6s valence orbital, while this effect is minor for copper and silver. Previous studies on the complexation of cationic coinage metal with ligands showed that the electrophilic character of the 6s orbital leads to the effective electron transfer in σ-donation (ligand → Au^+) and/or π-back-donation (Au^+ → ligand) with the fact that Au^+ toward close to the ligands.[22−27] Consequently, an increase covalent interaction contributes the binding between Au^+ and the ligands. Although the studied system is viewed as Au−furan$^+$, the relativity might play an influential role in driving electron transfer in Au−furan$^+$. A detailed theoretical analysis should provide a clearer answer for this issue. For the furan related complexes, Freiser and coworkers performed photodissociation by monitoring Co^+ fragment on Co^+−furan and determined BDE as 57 kcal/mol.[4] Stöckigt theoretically studied Al^+−furan, showing Al^+ lying over the furan ring with BDE = 29 kcal/mol.[5] As a result from the computational analysis, the interaction of Al^+ with furan is characterized by the existence of the σ-donation, but having a small amount of that electron transfer.

The theoretical approaches were employed to attain the complex geometries and to give a trend for the complex BDEs. MP2/6-31G(d, p) was used to fully optimize complex structures. For Cu and Ag, the complexes ended up with C_s symmetry, where the metals lie above the furan ring, as depicted in Figure 5. The Au/furan cationic complex exhibits a C_1 structure with the Au atom shifted outside the perimeter of the ring. A C_s symmetrical structure with gold lying over the furan resulted in one imaginary frequency and 5 kcal/mol less stable than a C_1 geometry at MP2 level. We cannot give the rational explanations for the structural discrepancy in Au complex at

TABLE 1: Structural Parameters (Å) of Metal/Furan Cationic Complexes Predicted at the MP2 Level of Theory

metal	ΔX^a	ΔY^a	R^b
Cu	0.659		1.951
Ag	0.677		2.309
Au		0.539	2.051

[a] The distance between the metal and the edge of the furan ring, referring to Figure 5. [b] The distance between the metal and the furan plane, referring to Figure 5.

TABLE 2: Binding Energies (kcal/mol) of Metal/Furan Cationic Complexes from Experimental and Theoretical Measurements

complex	method	D_0 (calcd)	D_0 (exptl)
Cu^+−furan	MP2/6-31G(d,p)	38.9	37
	CCSD(T)/6-31G(d,p)//MP2/6-31G(d,p)	37.6	
Ag^+−furan	MP2/6-31G(d,p)	25.9	28
	CCSD(T)/6-31G(d,p)//MP2/6-31G(d,p)	24.2	
Au^+−furan	MP2/6-31G(d,p)	58.4	62
	CCSD(T)/6-31G(d,p)//MP2/6-31G(d,p)	50.5	

this stage. The furan molecules were only slightly distorted for three complexes. In the previous studies in the complexation of the coinage cations with H_2O, both the Cu and Ag complexes reveal the ion−dipole forces resulting in a C_{2v} symmetry. The calculated geometry of Au/H_2O cationic complex deviates from the planar C_{2v} arrangement as the C_s structure, resulting from the relativistic effect accompanied with the re-hybridization of the H_2O molecule giving rise to the covalent contribution in the Au^+−H_2O bonding. Table 1 lists the structural data obtained from the MP2 calculations. As seen in Table 1, the vertical distances (***R***) from the metal atoms to the plane of the furan ring increase in the order copper < gold < silver. Regarding the complex BDEs, Table 2 shows the predictions from MP2 and CCSD(T) calculations. The experimental BDEs of the copper and silver complexes approximate the results in MP2 and CCSD(T) theoretical values. For the Au species, the CCSD-(T) was estimated by approximately 11 kcal/mol less than the energy measured experimentally. As the same was observed experimentally, either MP2 or CCSD(T) computations indicated the strong bond on the Au complex.

Au^+−C_3H_4. As seen in Figure 1, an intense peak assigned as Au^+−C_3H_4 stood up in the mass spectrum. We attempted to use both the photodissociation method and theoretical approach for inspecting the unknown C_3H_4 ligand. Photodissociation Au^+−C_3H_4 resulted in $C_3H_4^+$ formation with mass (*m*/*z*) 40, as illustrated in Figure 6a. Taking the assumption of C_3H_4 as allene, cyclopropene, or propyne, photodissociation action gave rise to charge-transfer mechanism from C_3H_4 to Au^+. The IE values are 9.62 eV for allene, 9.67 eV for cyclopropene, and 10.36 eV for propyne.[14,20] As stated earlier, photodissociation of Au−furan$^+$ led to $C_3H_4^+$ formation via a multiphoton absorption. Although both Au−furan$^+$ and Au^+−C_3H_4 species yield the same *m*/*z* 40, $C_3H_4^+$, peals, it is not certain whether both fragments represent the same structure. In particular, we have not conclusively determined the $C_3H_4^+$ identity in Au^+−C_3H_4 complex, as discussed below. Search the charge-transfer onset was conducted in order to yield the upper limit BDE. The threshold was located at 518 nm, where the $C_3H_4^+$ fragment was barely seen, and a structureless and continuously increased signal appeared as the scan moved toward the shorter wavelengths. The laser fluence 1.2 mJ/cm^2 was used throughout the experiment. Following the same procedure as utilized in the furan complexes, the threshold and ΔIE deduced the upper limits of the bond strength as 46 kcal/mol for Au^+−allene, 45 kcal/mol for Au^+−cyclopropene, and 29 kcal/mol for Au^+−propyne. The propyne complex appears quite low in BDE from our measurement. With the aid of the theoretical BDEs might facilitate an interpretation of the observed C_3H_4 channel.

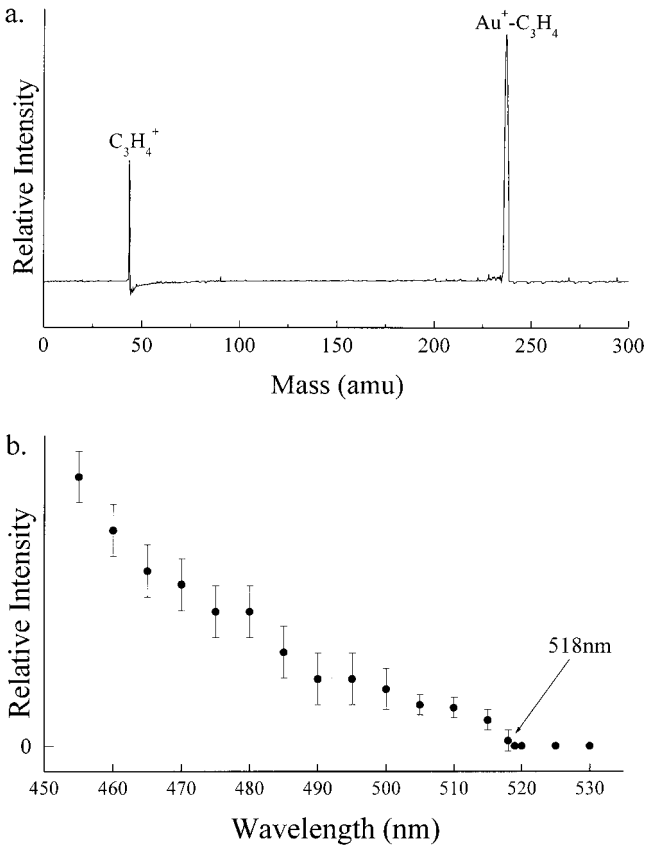

Figure 6. (a) Photodissociation mass spectrum of the mass-selected Au/C_3H_4 cationic complex at 355 nm with laser fluence of 5.6 mJ/cm^2; (b) Photofragment spectrum of Au/C_3H_4 cationic complex. Each data point was accumulated from two individual measurements and the average was taken. The arrow indicates the onset of the absorption band.

TABLE 3: Calculated Binding Energies (kcal/mol) for Au/C_3H_4 Cationic Complexes

C_3H_4	method	D_0 (calcd)
allene	MP2/6-31G(d,p)	56.0
	CCSD(T)/6-31G(d,p)//MP2/6-31G(d,p)	50.5
cyclopropene	MP2/6-31G(d,p)	53.9
	CCSD(T)/6-31G(d,p)//MP2/6-31G(d,p)	48.7
propyne	MP2/6-31G(d,p)	53.8
	CCSD(T)/6-31G(d,p)//MP2/6-31G(d,p)	50.1

In this respect the geometries of the Au^+−allene, Au^+−cyclopropene, and Au^+−propyne were fully optimized by MP2/6-31G(d, p) and the BDEs were further calculated using the CCSD(T) level of theory. It was found that gold atoms reside above the π-bonding C−C bonds as bridged structures in all three complexes. Table 3 gives the estimated values in BDEs. Computations suggest the approximate energies near 50 kcal/mol (CCSD(T)) for the proposed isomers. The experimental results in allene and cyclopropene are 4−5 kcal/mol slightly less than the predictions. The 29 kcal/mol derived in Au^+−propyne deviates significantly from the calculations. Therefore, allene and cyclopropene molecules seem to be possible candidates for C_3H_4 in our production. This consequence might conflict with the earlier studies in the pyrolysis of the free furan, where propyne was formed as the dominant fragment.[16] Lifshitz

and co-workers suggested the furan decomposition into allene as the major secondary product at the high temperature.[16] It is known that the laser ablation introduced here could readily create a high temperature plasma circumstance, which possibly makes the allene as the reaction exit channel. In any case, we cannot draw the definite conclusion for the C_3H_4 structure from these studies.

Finally, it should be mentioned that the further theoretical calculations using larger basis sets should give better predictions in the binding energies of the ion complexes containing furan and C_3H_4. Experimentally, two possible factors, internally hot ions and a two-photon excitation mechanism, leading to the incorrectly low experimental threshold need to be concerned. Using Ar as the carrier gas provides an opportunity to cool the vibrationally excited ions and improves the defined threshold. The results indicated that the onsets of the fragment appearance remained the same regardless of the gas properties for the studied complexes. Another possible contribution is that a two-photon absorption might take place at the photodissociation threshold. Dunbar and co-worker showed that one-photon behavior could occur if a small fraction of one-photon ions together with two-photon species presented in the threshold region.[28] The photofragment kinetic energy is the other uncertainty in the course of the complex dissociation. With the consideration of the kinetic shift resulting in the true onset appears toward the red.

Conclusion

From the viewpoint of the ionization energies, group 11 metal/furan cationic complexes are viewed as Cu^+-furan, Ag^+-furan, and Au$-$furan$^+$. With the presence of the gold atom resulting in the distinct reactions, giving the furan ring-opening channel C_3H_4. Although we refrained from a discussion on the metal reactivities, the enriched chemistry reveals the high reactivity of the gold center. Photodissociation performed on both Cu and Ag species gave rise to a charge-transfer behavior while Au complex occurred a simple bond cleavage. For Cu and Ag, calculations exhibited the metals lying above the furan ring with C_s structure. Interestingly, the gold atom was arranged outside the perimeter of the ring. The experimental BDEs are consistent with the theoretical predictions for Cu and Ag complexes, whereas the measured bond strength is 10 kcal/mol more than predicted value for Au species. Either the experimental or the theoretical measurements showed the enhanced binding energy in the Au/furan cationic complex. Increased bond strength might be involved in electron transfer between the metal and ligand, probably due to the relativistic effect in Au. Further theoretical analysis is needed to interpret this observation.

Experimental and theoretical approaches were also conducted to identify the possible C_3H_4 product, allene, cyclopropene, or propyne. Based on the BDE consideration, propyne is the molecule that shows the experimental value with the significant deviation from the theoretical value. From the previous studies of the furan decomposition at high temperature, allene is the possible candidate for C_3H_4, but the cyclopropene formation cannot be excluded completely.

Acknowledgment. The National Science Council of the Republic of China supported this work. We appreciate the helpful discussions with Dr. Ching-Han Hu concerning the theoretical calculations. Generous allocations of computational time at the National Center for High-performance Computing of the National Science are also acknowledged.

References and Notes

(1) See for example: (a) Dougherty, D. A. *Science* **1996**, *271*, 163. (b) Szilagyi, R. K.; Frenking, G. *Organometallics* **1997**, *16*, 4807. (c) Nicholas, N. J.; Hay, B. P.; Dixon, D. A. *J. Phys. Chem. A* **1999**, *103*, 1394.

(2) See for example: (a) Holzer, G.; Oro, J.; Bertsch, W. *J. Chromatogr.* **1976**, *126*, 771. (b) Lnul, T.; Tanabe, Y. *J. Catal.* **1978**, *52*, 375. (c) Lee, J. H.; Tang, I. N. *J. Chem. Phys.* **1982**, *77*, 4459. (d) Jones, A. *Chemistry of Heterocyclic Compounds*; Wiley: New York, 1990.

(3) Bakhtiar, R.; Jacobson, D. B. *J. Am. Soc. Mass Spectrom.* **1996**, *7*, 938.

(4) Nanayakkara, V. K.; Freiser, B. S. *J. Mass Spectrom.* **1997**, *32*, 475.

(5) Stöckigt, D. *J. Phys. Chem. A* **1997**, *101*, 3800.

(6) Gapeev, A.; Yang, C.-N.; Klippenstein, S.-J.; Dunbar, R. C. *J. Phys. Chem. A* **2000**, *104*, 3246.

(7) Su, P. H.; Yeh, C. S. *Chem. Phys. Lett.* **2000**, *331*, 420.

(8) Kershner, D. L.; Basolo, F. *Coord. Chem. Rev.* **1987**, *79*, 279.

(9) Yang, Y. S.; Yeh, C. S. *Chem. Phys. Lett.* **1999**, *305*, 395.

(10) Hay, P. J.; Wadt, W. R. *J. Chem. Phys.* **1985**, *82*, 299.

(11) Ehlers, A. W.; Böhme, M.; Dapprich, S.; Gobbi, A.; Höllwarth, A.; Jonas, V.; Köhler, K. F.; Stegmann, R.; Veldkamp, A.; Frenking, G. *Chem. Phys. Lett.* **1993**, *208*, 111.

(12) Frisch, M. J.; Trucks, G. W.; Schlegel, H. B.; Scuseria, G. E.; Robb, M. A.; Cheeseman, J. R.; Zakrzewski, V. G.; Montgomery, J. A., Jr.; Stratmann, R. E.; Burant, J. C.; Dapprich, S.; Millam, J. M.; Daniels, A. D.; Kudin, K. N.; Strain, M. C.; Farkas, O.; Tomasi, J.; Barone, V.; Cossi, M.; Cammi, R.; Mennucci, B.; Pomelli, C.; Adamo, C.; Clifford, S.; Ochterski, J.; Petersson, G. A.; Ayala, P. Y.; Cui, Q.; Morokuma, K.; Malick, D. K.; Rabuck, A. D.; Raghavachari, K.; Foresman, J. B.; Cioslowski, J.; Ortiz, J. V.; Stefanov, B. B.; Liu, G.; Liashenko, A.; Piskorz, P.; Komaromi, I.; Gomperts, R.; Martin, R. L.; Fox, D. J.; Keith, T.; Al-Laham, M. A.; Peng, C. Y.; Nanayakkara, A.; Gonzalez, C.; Challacombe, M.; Gill, P. M. W.; Johnson, B. G.; Chen, W.; Wong, M. W.; Andres, J. L.; Head-Gordon, M.; Replogle, E. S.; Pople, J. A. *Gaussian 98*, revision A.7; Gaussian, Inc.: Pittsburgh, PA, 1998.

(13) Moore, C. E. *Atomic Energy Levels;* National Bureau of Standards: Washington, DC, 1971.

(14) Herzberg, G. *Electronic Spectra and Electronic Structure of Polyatomic Molecules*; Van Nostrand Reinhold: New York, 1996.

(15) Grela, M. A.; Amorebieta, V. T.; Colussi, A. J. *J. Phys. Chem.* **1985**, *89*, 38.

(16) Lifshitz, A.; Bidani, M.; Bidani, S. *J. Phys. Chem.* **1986**, *90*, 5373.

(17) Organ, P. P.; Mackie, J. C. *J. Chem. Soc., Faraday Trans.* **1991**, *87*, 815.

(18) Fulle, D.; Dib, A.; Kiefer, J. H.; Zhang, Q.; Yao, J.; Kern, R. D. *J. Phys. Chem. A* **1998**, *102*, 7480.

(19) Liu, R.; Zhou, X.; Zuo, T. *Chem. Phys. Lett.* **2000**, *325*, 457.

(20) Parr, A. C.; Jason, A. J.; Stockbauer, R. *Int. J. Mass Spectrom. Ion Phys.* **1980**, *33*, 243.

(21) Pyykkö, P. *Chem. Rev.* **1988**, *88*, 563.

(22) Hrušák, J.; Schröder, D.; Schwarz, H. *Chem. Phys. Lett.* **1994**, *225*, 416.

(23) Hertwig, R. H.; Hrušák, J.; Schröder, D.; Koch, W.; Schwarz, H. *Chem. Phys. Lett.* **1995**, *236*, 194.

(24) Hrušák, J.; Hertwig, R. H.; Schröder, D.; Schwerdtfeger, P.; Koch, W.; Schwarz, H. *Organometallics* **1995**, *14*, 1284.

(25) Hertwig, R. H.; Koch, W.; Schröder, D.; Schwarz, H.; Hrušák, J.; Schwerdtfeger, P. *J. Phys. Chem.* **1996**, *100*, 12253.

(26) Lupinetti, A. J.; Fau, S.; Frenking, G.; Strauss, S. H. *J. Phys. Chem. A* **1997**, *101*, 9551.

(27) Schröder, D.; Schwarz, H.; Hrušák, J.; Pyykkö, P. *Inorg. Chem.* **1998**, *37*, 624.

(28) Dunbar, R. C.; Honovich, J. P. *Int. J. Mass Spectrom. Ion Processes* **1984**, *58*, 25.